

Design, fabrication, integration and commissioning of an upgraded guiding probe for the VLT unit telescope 4

Christoph Frank^a, Peter Hammersley^a, Bernard Buzzoni^a, Antonio Manescau*^a, Robin Arsenault^a, Pierre-Yves Madec^a, Martin Birkmann^a, Michael Mueller^a, Fernando Salgado^b, Stephane Guisard^b, Matthias Kroedel^c

^aEuropean Southern Observatory, Karl Schwarzschild Str. 2, 85748 Garching, Germany;

^bEuropean Southern Observatory, Paranal, Chile;

^cECM - Engineered Ceramic Materials GmbH, Am Bleichbach 12, 85452 Moosinning, Germany

ABSTRACT

As part of the preparation for the arrival of the MUSE instrument to the VLT, it was required to adapt the hosting telescope (UT4) guide probe, to increase its back focal length. This is to allow enough space for the later deployment of the MUSE Adaptive Optics module GALACSI, in-between the telescope adapter rotator and the instrument itself. The UT guide probe is a critical component for the successful operation of the telescope, so its modification to increase the telescope's back focal length, while maintaining full compatibility with the existing operation model and other hardware, was rather demanding.

The design, manufacture, assembly and test for the new supporting arm in the UT guiding probe is presented. It mixes the use of novel materials (HB-CESIC® for the mirrors substrates) and state of the art manufacturing techniques (3D printing mould production and rapid casting for the support structure), which allow producing easily a high performance subsystem. Characterization of the system prior delivery to the telescope, its integration in the UT and results after commissioning is presented. Its successful implementation has validated new manufacturing techniques that may prove very useful for future instruments development.

Keywords: optomechanics, telescope system, HB-CESIC

1. INTRODUCTION

Upgrade for existing subsystems in operation on telescopes, to improve or adapt performances, or as replacement for obsolete parts, is becoming more common. The design and development of such subsystems is rather challenging, as normally has to combine more demanding requirements than the subsystem to be replaced, with environmental, space, weight and other constraints. It is, however, possible to use new materials and manufacturing techniques, which were not available or considered at the time of the first design for the subsystems to replace.

The arrival of the MUSE instrument¹ to the VLT required adapting the unit telescope (UT) sensor arm to increase the telescope's back focal length. This change was necessary to keep space for the later deployment of the MUSE AO module GALACSI^{2,3}, which will be attached to the telescope adapter rotator and in front of the instrument itself. The change in the telescope back focal length requires the modification of the UT sensor arm⁴ such that this modification maintains full compatibility with the existing operation model of the telescope and other existing hardware.

Different alternatives were studied to carry out the modification but minimizing the modifications in the existing subsystems, such that if necessary it could be possible to step back and be able to restore the initial layout. The sensor arm was modified to compensate for the extra optical path, once it is increased the telescope back focal length. The design, manufacture, assembly, tests and commissioning for the new supporting arm in the UT sensor arm is detailed. The new sensor arm mixes the use of novel materials (HB-CESIC®⁵ for the mirrors substrates) with actual manufacturing techniques (molding and rapid casting for the support structure), which allowed producing a high performance subsystem where most of the manufactured parts, upon delivery, were almost ready to its integration. Characterization of the system prior delivery to the telescope, its integration in the UT and the commissioning results are presented.

*amanesca@eso.org; phone + 49 89 32006142; <http://www.eso.org>

2. THE VLT ADAPTER ROTATOR AND SENSOR ARM

A sensor arm unit is contained at each focal station of the VLT in its adapter rotator. It is a key element to maintain the telescope optical performance by providing several key functions for the normal operation of the UT such as the field acquisition, the guiding and the wavefront sensing. The photo below (Figure 1) shows a sensor arm in one UT Nasmyth adapter rotator.

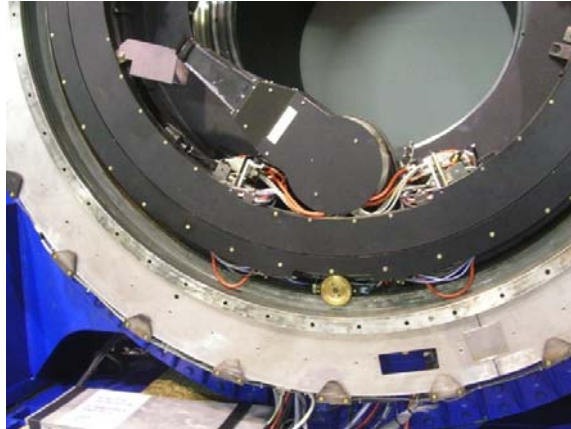


Figure 1. Photo of the sensor arm in the a VLT Nasmyth adaptor rotator

The sensor arm performs the three functions listed above, by using two sensors. The scheme of the arm is shown in Figure 2. It is equipped with an image camera and a wavefront sensor, which feedback the telescope active optics.

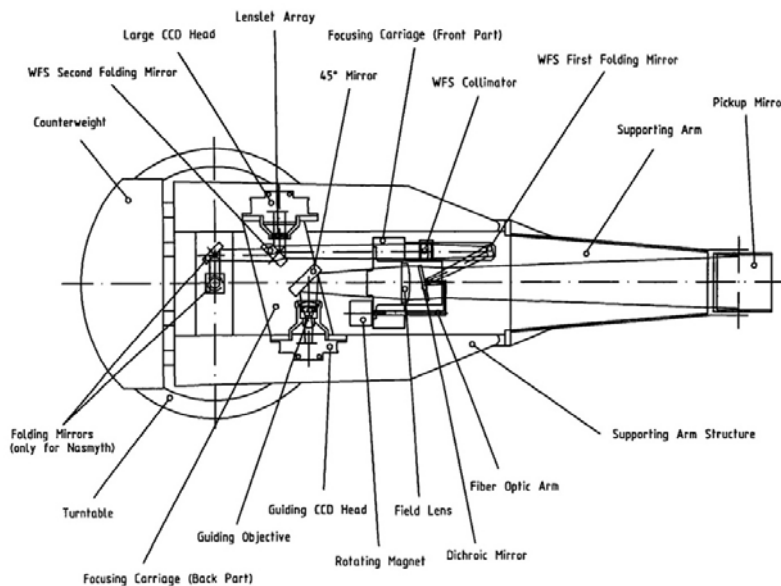


Figure 2. Layout and location of the principal components of the VLT sensor arm

3. INCREASE THE TELESCOPE BACK FOCAL LENGTH, THE SENSOR ARM DESIGN

In order to shift the location of the focal plane of the VLT by 250 mm backward (i. e. moving away from the Nasmyth rotator) it is proposed to translate the secondary mirror (M2) from its nominal position and to change the primary mirror (M1) profile (its conic constant) to correct for the spherical aberration. The modified telescope parameters are:

- Distance M1-M2: 12392.92 mm instead of 12396.429 mm
- M1 conic constant: -1.00562 instead of -1.00469
- Distance M3-Focus: 7050 mm instead of 6800 mm

With the above change in the prescription, which is feasible to be implemented, the curvature of the image is also modified and will be 2112.88 mm instead 2089.63 mm, in both cases with the concavity oriented towards the tertiary mirror. The rest of the parameters defining the telescope are as in its nominal prescription. The change does not affect the clear aperture of the reflective surfaces and the aperture stop of the system remains, as now, on the secondary mirror (with 1116 mm diameter).

It is important to remark that the telescope image scale is slightly changed and on axis it is 0.589 arcsec/mm (for the nominal telescope the image scale is 0.582 arcsec/mm); this difference is negligible.

To compensate for the increase of optical path, maintaining the sensor arm design, it has been decided to build a new supporting arm (see Figure 3 and 4). The scheme ray tracing for the new system is shown in Figure 3; it maintain the location of the pickup mirror (see Figure 2) and the use of two additional flat mirrors bend the beam to compensate for the change in the telescope back focal length.

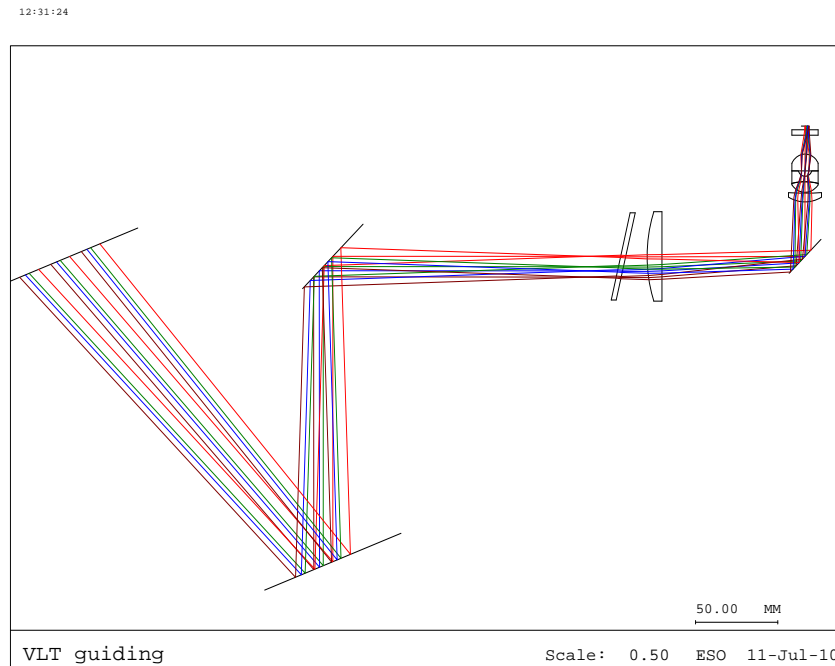


Figure 3. Ray tracing for the new sensor arm with the telescope prescription modified to increase the back focal length. Two extra flat mirrors help to add the extra 250 mm within the available envelope and maintaining the functions in the sensor arm

Even the new supporting arm is not that much different than the original one, a number of constraints have been taken into account for the design of the new one. In addition that the modified sensor arm shall fit in the constrained available space at the telescope's adapter rotator, other aspects such as weight, image movement, wavefront quality and thermal performance are key factors that shall be considered in the new design to allow the normal functioning for the telescope upon the change is implemented.

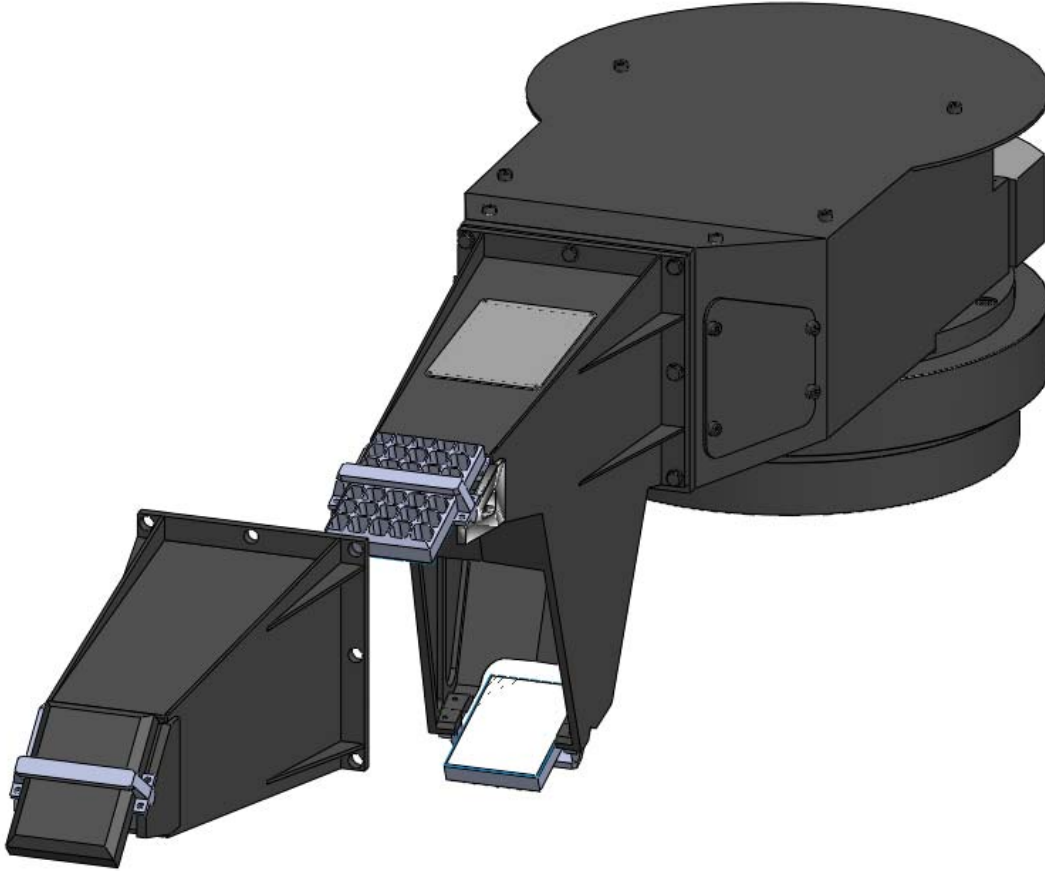


Figure 4. 3D view of the sensor arm with the new supporting arm attached to the main body (titanium structure); as comparison the original supporting arm is also shown

The weight for the new supporting arm is a key aspect in its design. The original supporting arm is made in Beryllium and weights 625 grams. As the new system is using two extra mirrors, it was unavoidable to increase the weight, however during its design it has been constrained by the proper selection of the materials and design. The final assembled new support arm weights 1062 grams and it is using lightweight HB-CESIC® mirrors installed in an optimized aluminum structure.

The optimized aluminum structure body provides performances both stiffness and thermal adequate for the use in the new supporting arm. Flexures from the mounting base of the arm extension to the tip of the pickup mirror amounts to about $4 \mu\text{m}$. The flexure over the full extent of the pickup mirror is $2.3 \mu\text{m}$. From thermal point of view the combination of the titanium (material used for the support arm structure and aluminum have a negligible change in focus within the normal temperature operation range. For the pupil the effect is also negligible.

The solution which is proposed assumes aluminum for the structure and HB-CESIC® for the mirrors. By using the estimated values for the aluminum the image displacement will go below 2.5 m-arcsec at the focal plane (image shift) and 0.011 % of pupil diameter in pupil plane (0.15 % is in the geometrical blur of the own pupil image). These values are negligible and will not impact the sensor arm performance.

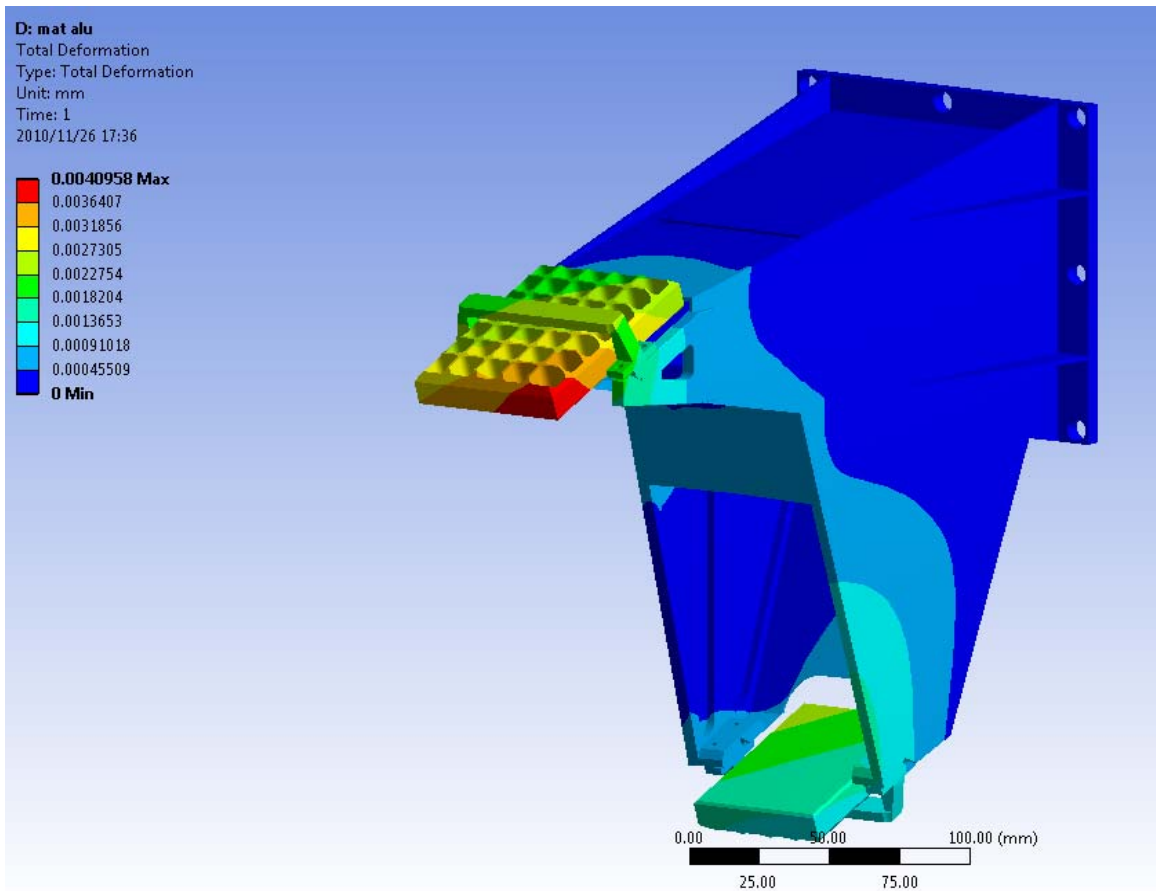


Figure 5. Flexure model for the new supporting arm, including mirrors. The material considered is aluminum

4. NEW SUPPORTING ARM MIRRORS

For the light weighted mirrors it was decided to use HB-CESIC®. This material offers extreme rigidity for a reasonable weight, which must resist deformation under their own weight. The greater the ratio between the material rigidity (Young Modulus) and the density, the higher the resistance. Below is presented a summary table comparing the properties for different materials considered for its use as mirror substrate.

As always an engineering design choice is a compromise between best performance and cost. Despite the great mechanical properties of Beryllium, it has been decided to exclude it given its manufacture complexity. Aluminum is simple, cheap and offers a good compromise. HB-CESIC® has been selected for the mirrors to ensure a safe, rigid behavior for the optics.

Table 1. Comparison of mechanical properties for some materials which potentially can be use din the pt submission.

| Material | Young modulus (GPa) | Density (g/cm3) | Intrinsic rigidity |
|-----------|---------------------|-----------------|--------------------|
| Aluminum | 69 | 2.64 | 26.1 |
| Beryllium | 287 | 1.84 | 156 |
| HB-CESIC® | 350 | 2.96 | 118 |
| Steel | 210 | 7.85 | 26.7 |
| Glass | ~80 | 2.58 | 31 |

Fabrication of light weighted HB-CESIC® mirrors offer the advantage that the mirror substrate can be manufactured in its final dimensions before it is infiltrated with silicon (very low shrinkage).

The optical quality of the mirrors in the sensor arm is important because they are in a location where the aberrations introduced cannot be measured and calibrated by the calibration source of the sensor arm; all the aberrations coming from the mirrors will be measured by the wavefront sensor and corrected by the active optics control. This would introduce a static aberration on the beam feeding the instrument and may reduce its final optical quality.

Engineered Ceramic Materials GmbH⁵ produced the mirrors. The manufacture includes several polishing runs using conventional techniques and are finished by using Magnetorheological Finishing (MRF) polishing to achieve the required optical (see Table 2).

Table 2. Measured surface quality of the one Pickup mirror. Similar measured surface quality has been measured for the other delivered mirrors

| Pickup mirror | | | |
|-------------------------------------|-----------------------------|----------------|-----------------|
| | Clear Aperture | PV (nm) | Rms (nm) |
| Specification | 79.00 x 54.00 mm | N/A | 80.0 |
| Measured as received | 77.20 x 56.16 mm | 244.2 | 28.02 |
| Measured after glued I/F | 77.20 x 56.16 mm | 246.8 | 29.02 |
| Pickup mirror (central area) | | | |
| Specification | 49.00 x 46.00 mm elliptical | N/A | 40.00 |
| Measured as received | 50.00 mm circular | 166.9 | 17.92 |
| Measured after glued I/F | 50.00 mm circular | 168.0 | 19.57 |

The mirror fixation and holding scheme has been designed to decouple the optical surface from the attachment. The Figure 6 show the mounting bridge, the mirror mounting and the mirror itself for the pickup mirror, together with a detail section for the mirror and mounting; the thin cut on top of the inserts decouple any possible stress induced by the screws from the mirror surface.

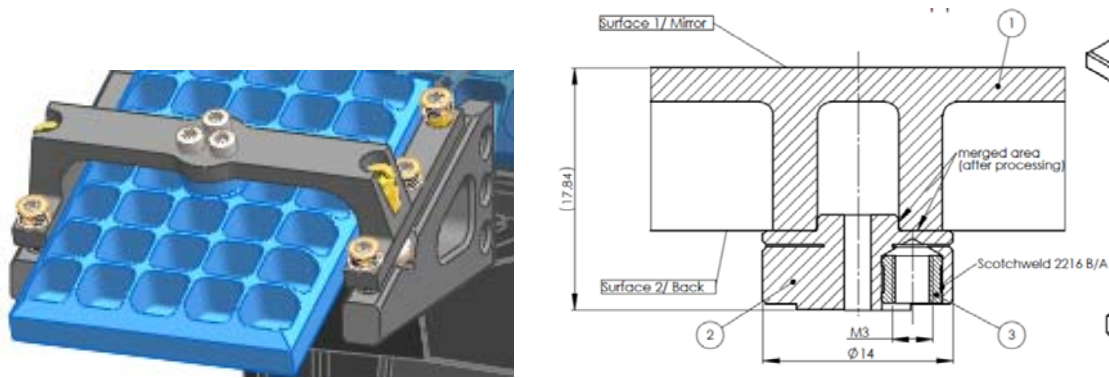


Figure 6. Attachment of the Pickup mirror to the bridge for its assembly. On the top right hand side it is shown the detail for the mounting fixation of the mirror to the bridge and on the top left the detail of the invar interface which decouples the attachment interface from the optical surface. The photo at the bottom shows the assembled pickup mirror; identical principle is used for all mirrors in the new supporting arm.

4.1 HB-CESIC® mirrors surface quality thermal performance

The correct performance with temperature is critical for the right operation of the sensor arm. The surface quality for the mirrors shall not be affected in the normal operation at the telescope. Even HB-CESIC® thermal properties are excellent it was decided to carry out surface quality vs. temperature test on one of the completed mirrors. In the next figure it is shown the experimental setup assembled in the thermal chamber and the measured surface quality at different temperatures from 5° to 20° C that basically is not affected.

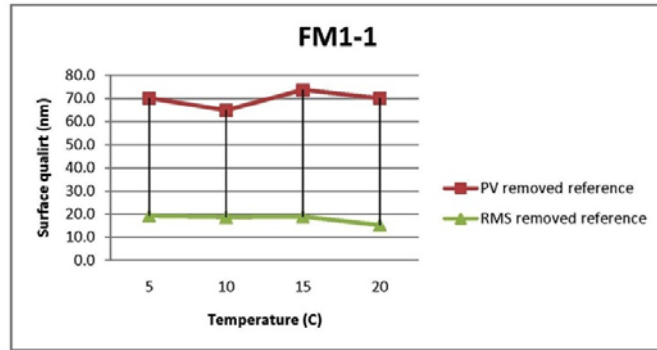
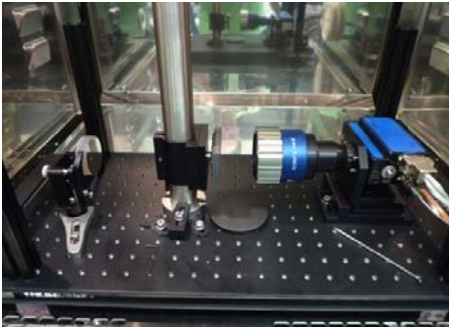


Figure 7. Measured surface quality for one of the mirrors for the new supporting arm between 5° and 20° C.

5. NEW SUPPORTING ARM STRUCTURE FABRICATION

Lightweight is a major requirement in the design for the new supporting arm. Fabrication process shall be considered as well during the design; this brings to consider state of the art production technology with well-known materials. Although 3D-printing technology is available since the 90's it is now when is becoming to be more frequent in production. It is a flexible technique that allows the reduction of production cost and enables the manufacturing of parts not possible otherwise. Several schemes have been developed: Fused deposition modeling, Laser sintering, Electron-beam melting, Laminated object modeling Stereolithography and more. Access of the general public to 3D-printers has been hindered by the high cost of such devices, but the expiration of key patents in February 2014 is resulting in a major investment of companies to produce cheaper, more affordable machines for the general public.

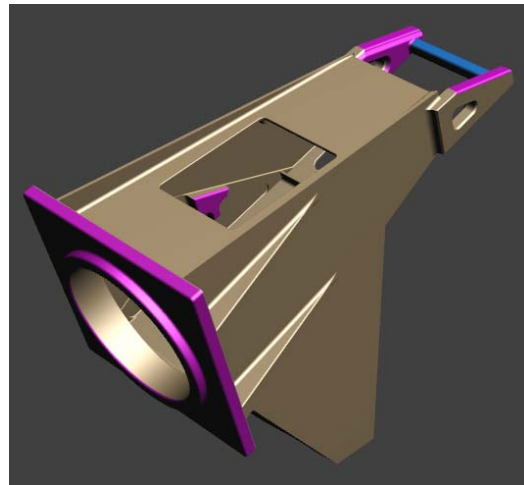
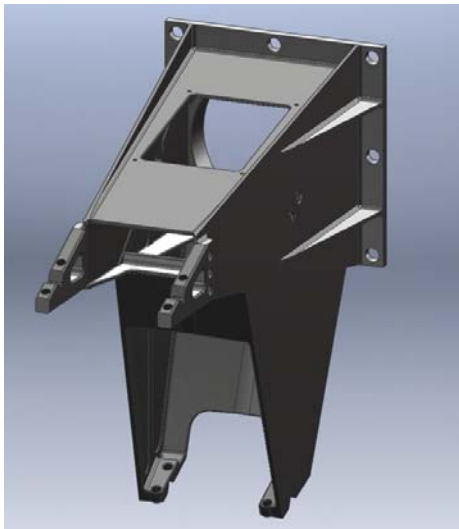


Figure 8. The first step of production is a Computer Aided Design of the part to be manufactured. On the left hand side the designed piece and below is shown the one prepared with the specific modifications for the casting process

3D-printing is a master forming process which is also known as additive manufacturing technique, opposed to retrieval standard machining techniques, where a big block of material (steel, aluminum, etc.) is drilled and milled in order to remove material until the desired shaped is reached. Additive manufacturing may be the only way where it is possible manufactures complex and intricate shapes and parts. This technique has been used for the fabrication of the structure of the new supporting arm and the extension flange for the VLT test camera (see section 8).

The new supporting arm structure is a monolithic piece, providing high rigidity; a conventional manufacturing could be done but shall be done in several parts that will be assembled latter. Bolts and nuts would be required, which would weaken the part and make the performance simulation (Finite Element Modeling) more complex and less reliable. This is the reason why it was decided to use 3D printing to produce the mold, which was later on used to cast the part. However, the particle deposited in layers, which are bonded together with a biding agent produces a PMMA (Polymethylmethacrylate; thermoplastic); this material is far too weak to be usable in the final part. Voxeljet AG⁶ has developed a way to produce a mold doesn't fit out of this part to end the process with a metal casting.



Figure 9. The PMMA part manufactured by 3D-printing (Illustrative models on the top). The Wax infiltrated model is then processed to produce a ceramic mold. Then the chosen metal is casted in the mold (in this case Aluminum G-AlSi10Mg T6). The final result is shown on the bottom right. The remaining steps to complete the part manufacture include the thermal treatment and a conventional machining of some surfaces, which required high accuracy as are used for interfaces

6. INTEGRATION, ALIGNMENT AND TEST

The integration, alignment and test were performed before delivery to the observatory. Appropriate toolings, with the right references were designed and procured. A key element in the integration, alignment and test has been the integration stand (see photo in Figure 10), which was designed tailored to the processes required to assess the system completion; it includes an attachment surface with the same definition as in the existing sensor arm. The compensation and alignment strategy benefit from the system sensitivity analysis for image movement.



Figure 10. Partially integrated new supporting arm on the integration stand.

6.1 Transmitted wavefront

Overall estimation of the transmitted wavefront was measured setting the system in front of an interferometer and illuminating the assembly with a flat wavefront. Notice that in operation the system is illuminated with $\sim F/15$ convergent beam. The clear aperture of the last mirror limited illumination clearance, however as the results are well within the required maximum error and the known individual mirror surface quality. Transmitted wavefront error shall be better than 260 nm rms; measured wavefront error was 50 nm rms over a clear aperture of 50x56 mm. The photo in Figure 11 shows the system during the transmitted wavefront error measurements.

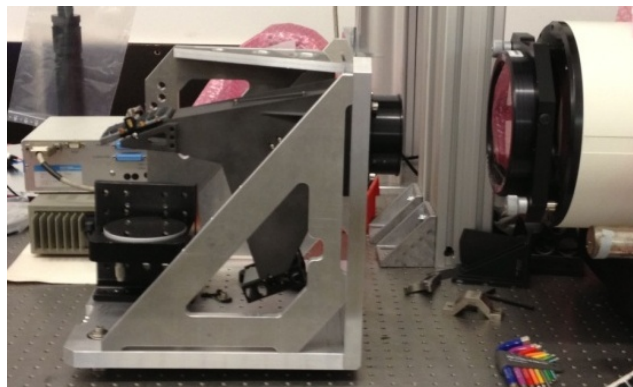


Figure 11. Fully integrated new sensor arm in the integration stand set in front of the interferometer transmitted wavefront error measurement

6.2 Image movement

Again with the help of the integration stand and mounting on a rotary stage it was performed measurements of the image movement. A laser alignment sensor mounted at the nominal telescope image plane was used to detect shift and tilts for different orientations from -90° to $+70^\circ$. The photos in Figure 12 show the system while the measurements for two different orientations. Results are summarized in the Figure 13; note that maximum displacement requirement is ± 150 microns.

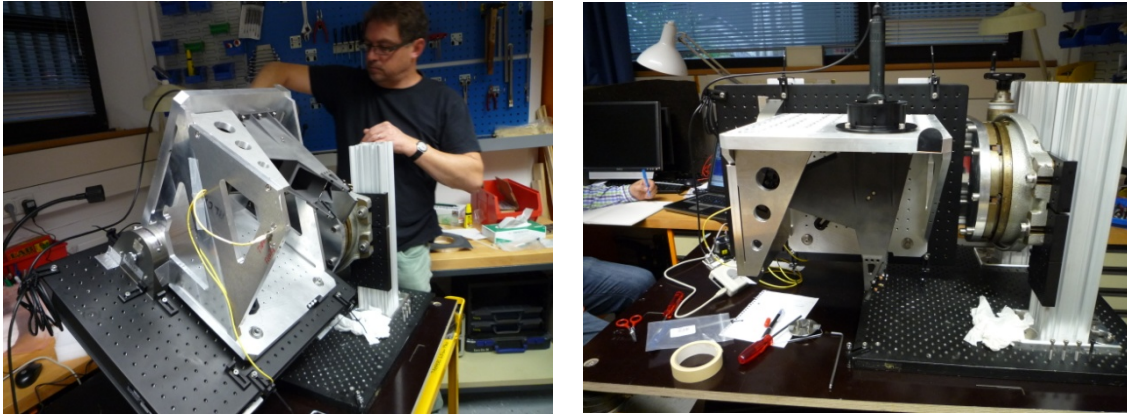


Figure 12. Supporting arm on the integration stand while performing the image movement tests

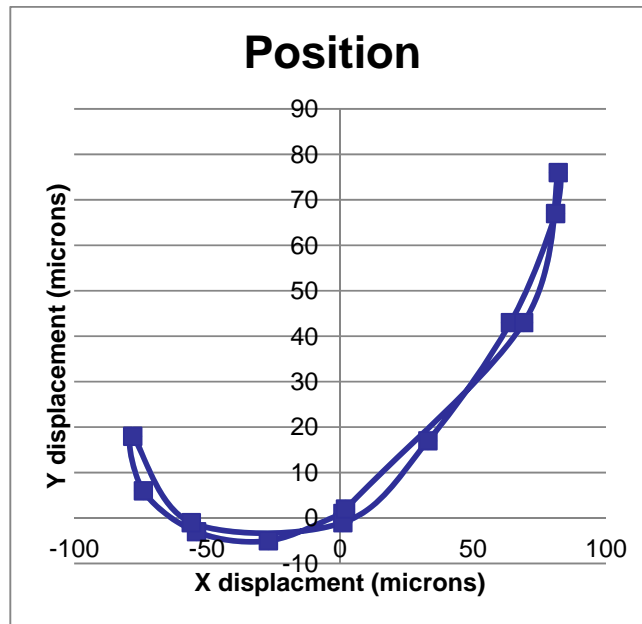


Figure 13. Measurements for image displacement for orientations between -90° to $+70^\circ$

7. INSTALLATION IN TELESCOPE

Upon completion its integration and test, the system was delivered to the Paranal observatory for installation. Proper transport boxes were prepared and the system was checked for correct alignment before proceeding with the installation. The original supporting arm was removed from the sensor arm and was installed in the test stand to set baseline alignment reference to which was finally adjusted the new support arm. Once the new support arm was checked against this baseline the new support arm was installed in the sensor arm.



Figure 14. Photo taken while the installation of the new supporting arm on the sensor arm. Once removed the original sensor arm and checked space and interfaces it continued the installation.

The end switches of the guiding camera focusing table were adjusted and it was added an extra counterweight of 1.9 kg on top of the existing one, to properly balance the upgraded sensor arm. Coarse alignment was performed using the sensor arm wavefront sensor illuminated with a laser beacon that is installed in the center of the telescope secondary mirror.



Figure 15. The new supporting arm installed on the sensor arm at the Nasmyth adapter rotator of UT4

8. COMMISSIONING

The 3D-printing technology was used to manufacture a larger and robust component, required for the commissioning of the new sensor arm. The VLT test camera was used as reference and then for the test with the new telescope configuration, a proper interface with the adapter rotator was needed. An extension flange was designed to adapt the VLT test camera to the new focal position. This part was manufactured in record time by the company ACTech GmbH⁷ by using 3D-printing methods. The main advantages for this type of structure are: again a high rigidity due to the monolithic and homogeneous nature of the cast, and a simpler and more reliable thermal stress relief usually very delicate for the usual mechanically-welded scheme typically used to produce this kind of structures.

There were two commissioning periods: one following the installation of the new support arm between October 28th and November 3rd, 2013 and a second period from January 8th to 10th, 2014 where it was confirmed the correct operation of the modified sensor arm following the changes made, when converting from the original to one with an increased distance from the pickup mirror to the focal plane. Tests were made both before and after the support arm was changed so the performance could be compared.

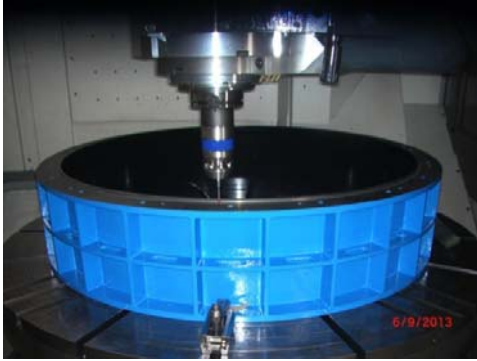


Figure 16. On the left it is shown the extension flange verification at the manufacturer premises. On the right the ~1.2m diameter spacer to install the VLT test camera at the proper focal plane position (extended by 250mm) at the Nasmyth focus.

The important results for the commissioning are:

- The focal plane has moved back 250 mm (± 2.5 mm measurement error)
- The refocusing range for the guiding / wavefront sensor has decreased from 99 mm to 90 mm. It has not impact on the operation and performance of the system
- As predicted vignetting in the field of view of the guide camera is detected, however there is no vignetting at the position of the dichroic so it do not affect the wavefront sensor performance
- The reference pixel for the guide camera was adjusted so that the position is well within the good part of the dichroic
- The plate scale has changed by a factor 0.986 as expected
- The transmission of the new arm is 75% that of the original arm, as expected
- The guiding and telescope wavefront sensors work as expected. A new ONECAL look up table has been built and installed
- The guide probe astrometric calibration was made and the calibration seems to be stable between November 2013 and January 2014
- Telescope image quality is acceptable; images on the test camera of less than $0.4''$ were obtained
- The tracking and offsetting measured appear to be as expected. The offsetting accuracy seems to be limited by the guide probe calibration, $\sim 0.2\%$ of the offset with a repeatability of ~ 20 mas

9. CONCLUSION

The upgrade of the Unit Telescope 4 Nasmyth B sensor arm has been completed successfully, allowing the installation of the MUSE instrument. A new supporting arm structure was designed and manufactured using novel materials and fabrication methods, which have demonstrated to be reliable, fast and cost effective in the design of high performance subsystems. High quality lightweight HB-CESIC® mirrors have been produced, tested and integrated. 3D printing opens a new paradigm where such parts (one-off's) can be produced much more economically and fast.

Acknowledgments

We would like to thank the staff at Paranal Observatory for their support during the installation and commissioning.

REFERENCES

- [1] Bacon, R., et al., "The MUSE second-generation VLT instrument", Proc. SPIE 7735, 773508 (2010)
- [2] Stroebele, S., et al., "GALACSI System Design and Analysis", Proc. SPIE 8447, 844737 (2012)
- [3] La Penna, P., Stroebele, S., Aller-Carpentier, E., Argomedo, J., Arsenault, R., Conzelmann, R. D., Delabre, B., Donaldson, R. H., Duchateau, M., Fedrigo, E., Gago Rodriguez, F., Hubin, N., Quentin, J., Jolley, P. D., Kiekebusch, M., Kirchbauer, J.-P., Klein, B., Kolb, J., Kuntschner, H., Le Louarn, M., Lizon L'Allemand, J.-L., Madec, P.-Y., Manescau, A., Mehrgan, L. H., Suarez Valles, M., Soenke, Ch. and Tordo, S., "GALACSI integration and functional tests", Proc SPIE 9148, 9148101 (2014)
- [4] Salgado, F., Haddad, J., Hudepohl, G. and Medina, R., "Success of long-term preventive maintenance on telescope subsystems using the example of the VLT adapter-rotators at the ESO Paranal Observatory", Proc. SPIE 8448, 844825 (2012)
- [5] <http://www.cesic.de/>
- [6] <http://www.voxeljet.de/>
- [7] <http://www.actech.de/>